Acta Crystallographica Section F
Structural Biology and Crystallization Communications
ISSN 1744-3091

Crystallization and preliminary diffraction analysis of the CAL PDZ domain in complex with a selective peptide inhibitor

Jeanine F. Amacher, Patrick R. Cushing, Joshua A. Weiner and Dean R. Madden*

Department of Biochemistry, Dartmouth Medical School, 7200 Vail Building, Hanover, NH 03755, USA

Correspondence e-mail: drm0001@dartmouth.edu

Received 1 February 2011
Accepted 16 March 2011

Cystic fibrosis (CF) is associated with loss-of-function mutations in the CF transmembrane conductance regulator (CFTR), which regulates epithelial fluid and ion homeostasis. The CFTR cytoplasmic C-terminus interacts with a number of PDZ (PSD-95/Dlg/ZO-1) proteins that modulate its intracellular trafficking and chloride-channel activity. Among these, the CFTR-associated ligand (CAL) has a negative effect on apical-membrane expression levels of the most common disease-associated mutant ΔF508-CFTR, making CAL a candidate target for the treatment of CF. A selective peptide inhibitor of the CAL PDZ domain (iCAL36) has recently been developed and shown to stabilize apical expression of ΔF508-CFTR, enhancing net chloride-channel activity, both alone and in combination with the folding corrector corr-4a. As a basis for structural studies of the CAL–iCAL36 interaction, a purification protocol has been developed that increases the oligomeric homogeneity of the protein. Here, the co-crystallization of the complex in space group $P2_12_12_1$, with unit-cell parameters a = 35.9, b = 47.7, c = 97.3 Å, is reported. The crystals diffracted to 1.4 Å resolution. Based on the calculated Matthews coefficient (1.96 Å^3 Da^{-1}), it appears that the asymmetric unit contains two complexes.

1. Introduction

The cystic fibrosis transmembrane conductance regulator (CFTR) is an epithelial chloride channel that is defective in patients with cystic fibrosis (CF). A number of proteins regulate its post-maturational localization and trafficking to and from the membrane (Guggino & Stanton, 2006). These include the Na^+/H^+-exchanger regulatory factors NHERF 1, NHERF2, NHERF3 and the CFTR-associated ligand (CAL). Each of these proteins contains one or more PDZ (PSD-95/Dlg/ZO-1) domains, modular protein-interaction elements which constitute one of the most common families in the human genome. Typically, a given PDZ domain is capable of binding a number of target proteins at their carboxy-termini. Conversely, as with CFTR, a PDZ-binding protein often interacts with multiple PDZ domains (Harris & Lim, 2001; Nourry *et al.*, 2003).

The PDZ binding partners of CFTR have distinct effects on its intracellular trafficking and net chloride-channel activity. Among them, CAL is the only PDZ partner that has been shown by over-expression and RNA interference studies to have a clear negative effect on the apical-membrane abundance of CFTR (Cheng *et al.*, 2002; Wolde *et al.*, 2007). Peptide engineering identified a peptide inhibitor (iCAL36) that binds the CAL PDZ domain at least 170-fold more tightly than any of the NHERF domains and significantly enhances ΔF508-CFTR chloride efflux in polarized patient-derived airway epithelial cells (Cushing *et al.*, 2010; Vouilleme *et al.*, 2010). Although heteronuclear single-quantum coherence experiments demonstrate that iCAL36 occupies the CAL PDZ peptide-binding cleft (Cushing *et al.*, 2010), they do not provide detailed three-dimensional information about the complex. Thus, in order to visualize the stereochemical basis of the high-specificity CAL–iCAL36 interaction, we now report a CAL PDZ purification protocol that permits cocrystallization and preliminary diffraction analysis of the domain in complex with the iCAL36 peptide.

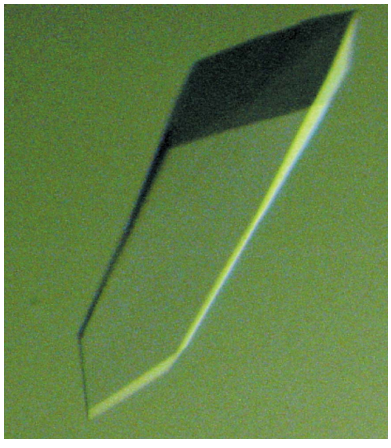

© 2011 International Union of Crystallography
All rights reserved

2. Materials and methods

2.1. Protein expression and purification

A CAL PDZ construct (CALP) was engineered in the pET16b backbone. Following the vector decahistidine tag, the expressed sequence includes a linker (SSGHIEGRHM), a cleavage site for the human rhinovirus 3C protease (LEVLFQ*GP) and the CAL PDZ domain (residues 278–362; UniProt accession No. Q9HD26-2). CALP was expressed in *Escherichia coli* BL21 (DE3) RIL cells in 2×YT medium containing 100 µg ml^{-1} ampicillin and 34 µg ml^{-1} chloramphenicol. At an OD_{600} of 0.6–0.8, 0.1 m*M* isopropyl *β*-D-1-thiogalactopyranoside was added. Following induction, cells were grown for 18 h at 289 K and harvested by centrifugation.

Cell pellets were resuspended in 50 ml lysis buffer [50 m*M* Tris pH 8.5, 150 m*M* NaCl, 1 m*M* dithiothreitol (DTT), 2 m*M* $MgCl_2$, 1 m*M* ATP, 5 µl Benzonase (EMD), one Complete EDTA-free tablet (Roche)] per litre of culture and lysed by passage through a French press three times at ∼80 MPa. The lysate was clarified by ultracentrifugation in a Ti45 rotor (60 min, 125 000*g*, 277 K). The supernatant was supplemented with 10 m*M* imidazole and loaded onto a Qiagen Ni–NTA Superflow column pre-equilibrated with Ni–NTA buffer (50 m*M* Tris pH 8.5, 150 m*M* NaCl, 1 m*M* DTT, 1 m*M* ATP) containing 10 m*M* imidazole. The column was washed with 20 column volumes (CV) of Ni–NTA buffer containing 10 m*M* imidazole and 3 CV of Ni–NTA buffer containing 35 m*M* imidazole. Bound proteins were eluted using a linear gradient from 280 to 400 m*M* imidazole. Eluates were collected in 4 ml fractions in test tubes containing 20–30 mg Chelex 100 Molecular Biology grade resin (Bio-Rad) and 250 mmol ethylenediaminetetraacetic acid pH 8.0.

CALP-containing fractions were pooled, centrifuged at 600*g* for 10 min to pellet the Chelex resin and loaded onto a HiLoad 26/60 Superdex S75 size-exclusion chromatography (SEC) column (GE Healthcare) in GF1 buffer [50 m*M* Tris pH 8.5, 150 m*M* NaCl, 0.02%(*w*/*v*) sodium azide, 1.5 m*M* tris(2-carboxyethyl)phosphine (TCEP), 1 m*M* ATP, 1 m*M* glutamate, 2 m*M* $MgCl_2$, 5%(*v*/*v*) glycerol]. The N-terminal decahistidine tag was cleaved from the pooled CALP fractions using human rhinovirus 3C protease (Novagen) at a protein:protease mass ratio of 50:1 overnight at 277 K.

Cleaved CALP was supplemented with 20 m*M* imidazole and recovered using a 5 ml HisTrap HP (GE Healthcare) column pre-equilibrated with Ni–NTA buffer containing 20 m*M* imidazole and 0.02%(*w*/*v*) sodium azide. The flowthrough volume was collected and 5 CV of equilibration buffer were used to wash out residual unbound CALP protein. The cleaved CALP was concentrated using a stirred cell with a YM-1 membrane and loaded onto a Superdex S75 column equilibrated in GF2 buffer [25 m*M* Tris pH 8.5, 150 m*M* NaCl, 0.02%(*w*/*v*) sodium azide, 0.1 m*M* TCEP, 0.1 m*M* ATP, 5%(*v*/*v*) glycerol]. The purity of the resulting fractions was assessed by SDS–PAGE. Fractions containing CALP were pooled and concentrated using a stirred cell with a YM-1 membrane. CALP was dialyzed overnight in 150 m*M* NaCl, 0.02%(*w*/*v*) sodium azide, 25 m*M* sodium phosphate pH 8.0, 0.2 m*M* TCEP, 5%(*v*/*v*) glycerol.

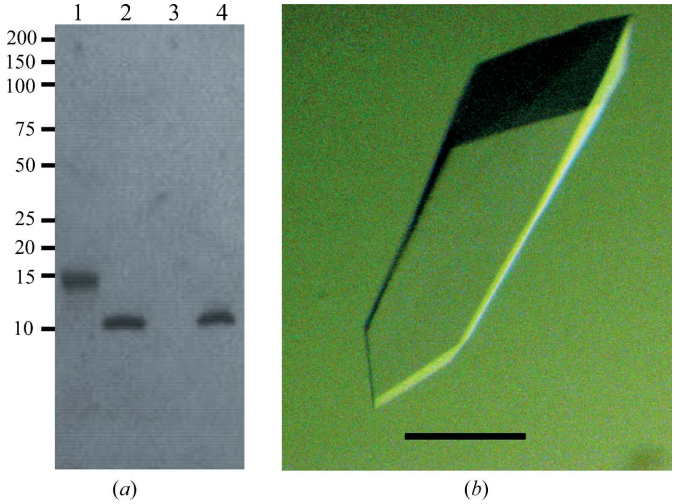

Figure 1
Purification and crystallization of CALP and cocrystallization with iCAL36. (*a*) Silver-stained SDS–PAGE showing a protein with the expected mass for CALP before (lane 1) and after (lane 2) removal of the polyhistidine tag by human rhinovirus 3C protease. Following serial washes, samples of mother liquor (lane 3) or a crystal (lane 4) were dissolved in sample buffer. SDS–PAGE demonstrates the presence of CALP in the crystal (lane 4) but not in the control (lane 3). The relative molar masses of standard proteins are shown to the left of the standard bands in kDa. (*b*) A representative crystal of CALP–iCAL36 is shown. The scale bar represents 0.1 mm.

2.2. Crystallization of the CAL PDZ domain

For crystallization trials, CALP was dialyzed into screening buffer (10 m*M* HEPES pH 7.4, 25 m*M* NaCl) and adjusted to a final concentration of 5.5 mg ml^{-1}. iCAL36 (sequence ANSRWPTSII) was added to a final concentration of 1 m*M*, yielding a protein:peptide molar ratio of ∼1:1.7. Initial conditions for cocrystallization of the CALP–iCAL36 complex were obtained by microbatch screening at the Hauptman–Woodward Institute High-Throughput Screening laboratory (Luft *et al.*, 2003). Candidate crystallization conditions were optimized in hanging-drop format at 291 K. For these experiments, a solution consisting of 5.5 mg ml^{-1} CALP and 1 m*M* iCAL36 was mixed in a 1:1 ratio with reservoir solution to give a total volume of 4 µl and was allowed to equilibrate by vapor diffusion against a 500 µl reservoir. Crystals appeared in 2–4 d and continued to grow for up to 10 d. The crystal used for the native diffraction experiment described below was obtained using 300 m*M* KBr, 100 m*M* Tris pH 8.0, 30%(*w*/*v*) polyethylene glycol (PEG) 8000 as reservoir buffer.

Crystal content was analyzed by SDS–PAGE as well as by matrix-assisted laser desorption/ionization time-of-flight (MALDI–TOF) mass spectrometry. The crystal used for SDS–PAGE analysis was grown using a reservoir buffer consisting of 100 m*M* NaCl, 100 m*M* Tris pH 7.5, 32%(*w*/*v*) PEG 8000. The crystal dimensions were approximately 100 × 100 × 600 µm. The crystal used for MALDI–TOF analysis was obtained using 100 m*M* NaCl, 100 m*M* Tris pH 7.5, 31%(*w*/*v*) PEG 8000 as the reservoir buffer. Its dimensions were approximately 100 × 200 × 500 µm. Each crystal was washed by four serial transfers through 50 µl drops of fresh reservoir buffer. For SDS–PAGE, the crystal was transferred into 50 µl tricine sample buffer. For MALDI–TOF, the crystal was transferred to 50 µl water. As controls, additional samples were prepared in parallel from samples of mother liquor following the same wash protocol.

Following SDS–PAGE, proteins were visualized by silver staining (Fig. 1*a*). For MALDI–TOF, additional controls included 10 µl samples containing 3 µg of either CALP or iCAL36. Samples were desalted following the OMIX protocol (Varian Inc). Briefly, a 10 µl OMIX tip was washed in 50%(*v*/*v*) acetonitrile. The tip was then equilibrated using 0.1%(*v*/*v*) trifluoroacetic acid (TFA), after which a 50 µl sample was loaded and washed using 0.1%(*v*/*v*) TFA. Samples were eluted directly onto a MALDI–TOF plate using sinapinic acid. Data were collected on a Voyager-DE PRO MALDI–TOF (PE Biosystems) instrument operating at 25 000 V using a bin size of 2 ns.

2.3. Data collection and analysis

For diffraction screening and data collection, a crystal was transferred into cryoprotectant buffer [300 m*M* KBr, 100 m*M* Tris pH 8.0, 30%(*w*/*v*) PEG 8000, 20%(*v*/*v*) glycerol] and subsequently flash-cooled by plunging it into a liquid-nitrogen bath. Crystal diffraction was evaluated at 100 K on beamline X6A at the National Synchrotron Light Source (NSLS) at Brookhaven National Laboratory. Native oscillation data were collected at λ = 0.91810 Å over a 360° range, using 1° frames and an exposure time of 10 s per frame. Data were processed using the *XDS* package (Kabsch, 2010; see Table 1). Molecular-replacement studies were performed using *PHENIX* (Adams *et al.*, 2010; McCoy, 2007), using apo and CFTR-bound CALP NMR structures as search models, and *BALBES* (Long *et al.*, 2008), using search models with PDB codes 1q3o (Im *et al.*, 2003), 1qau (Hillier *et al.*, 1999), 2ego (Sugi *et al.*, 2007), 3cby (Zhang *et al.*, 2009), 1kwa (Daniels *et al.*, 1998) and 2gwb (Piserchio *et al.*, 2005).

3. Results and discussion

We have previously reported the biochemical and NMR structural analysis of a CAL PDZ domain that was purified with its decahistidine tag intact (Wolde *et al.*, 2007; Piserchio *et al.*, 2005; Cushing *et al.*, 2008). However, this protein exhibited a strong tendency to aggregate at pH <8.0, as established by analytical SEC and NMR experiments (Piserchio *et al.*, 2005). Several factors suggested that the tendency to aggregate was associated with the presence of the decahistidine purification tag, possibly involving chelation of residual metal ions in solution. In particular, analytical SEC data revealed that aggregation was reduced by the inclusion of metal chelators in the fraction-collection tubes for the initial Ni–NTA chromatography capture step. As a result, we hypothesized that post-capture proteolytic cleavage of the decahistidine tag could produce a construct that was more amenable to crystal structure analysis.

To test this hypothesis, we engineered a CALP construct with a human rhinovirus 3C protease cleavage site following the N-terminal decahistidine tag. Purification and proteolytic cleavage with human rhinovirus 3C protease yielded protein of high purity (Fig. 1*a*, lane 2). Analytical SEC confirmed the oligomeric homogeneity (>97%) of the purified protein even at concentrations of >10 mg ml^{-1} (data not shown).

The initial crystallization conditions identified by microbatch screening (Luft *et al.*, 2003) were reproduced and optimized by hanging-drop vapor diffusion (Fig. 1*b*). The identity of the crystallized complex was verified using SDS–PAGE and MALDI–TOF analysis. A silver-stained gel of a washed crystal showed a single band corresponding to the molecular weight of cleaved CALP (Fig. 1*a*, lane 4). The negative-control sample (washed mother liquor) showed no bands (Fig. 1*a*, lane 3), confirming the efficiency of the washing protocol. To verify the presence of the peptide, MALDI–TOF analysis was also performed on a washed crystal. The resulting spectrum showed two major peaks at 1131.3 ± 0.5 Da, corresponding to iCAL36 (calculated MW of 1144 Da), and at 9343 ± 2 Da, corresponding to CALP (calculated MW of 9339 Da). Similar peaks were also seen in a control sample of CALP–iCAL36 in crystallization buffer at 1159 ± 12 Da and 9336 ± 6 Da, respectively. The negative-control sample (washed mother liquor) showed only a background curve with no major peaks (data not shown).

The diffraction data exhibited Bragg reflections that were visible to at least 1.5 Å resolution (Fig. 2). A full native diffraction data set was collected and processed to a resolution of 1.4 Å ($R_{\rm merge}$ = 0.035; see Table 1). The CALP–iCAL36 complex crystallized in space group $P2_12_12_1$. Resolution-dependent Matthews coefficient probability analysis (Kantardjieff & Rupp, 2003) suggested the presence of two molecules per asymmetric unit, yielding a $V_{\rm M}$ of 1.96 Å^3 Da^{-1}, with 37% solvent content.

Table 1
Crystallographic and data-collection statistics.

Values in parentheses are for the highest resolution shell.

Space group	$P2_12_12_1$ [No. 19]
Unit-cell parameters (Å)	a = 35.88, b = 47.71, c = 97.31
Matthews coefficient (Å^3 Da^{-1})	1.96
Molecules per asymmetric unit	2
Solvent content (%)	37
Wavelength (Å)	0.91810
Resolution (Å)	48.65–1.4 (1.47–1.4)
Unique reflections	33705 (5074)
$R_{\rm merge}$†	0.035 (0.146)
$\langle I/\sigma(I)\rangle$	42.90 (11.5)
Completeness (%)	99.9 (99.8)

† $R_{\rm merge} = \sum_{hkl}\sum_i |I_i(hkl) - \langle I(hkl)\rangle| / \sum_{hkl}\sum_i I_i(hkl)$, where $I_i(hkl)$ and $\langle I(hkl)\rangle$ are the ith and the mean measurements of the intensity of reflection hkl.

Molecular-replacement studies failed to yield compelling solutions using either *PHENIX* (Adams *et al.*, 2010; McCoy, 2007) or *BALBES* (Long *et al.*, 2008). Search models included the solution structure of the CAL PDZ domain in the unbound state (Piserchio *et al.*, 2005; Li *et al.*, 2006) or bound to a CFTR C-terminal peptide (Piserchio *et al.*, 2005), as well as crystal structures of PDZ domains with sequence similarity identified by the *BALBES* search algorithm. OMIT maps were computed for a number of candidate solutions, but none of them exhibited electron density for the omitted regions. As a result, although alternative molecular-replacement strategies may be successful, structure determination is likely to require experimental phase information. Independent of the final phasing strategy, the approach presented here provides the first high-resolution diffraction data from a crystal of the CAL PDZ domain and the presence of the

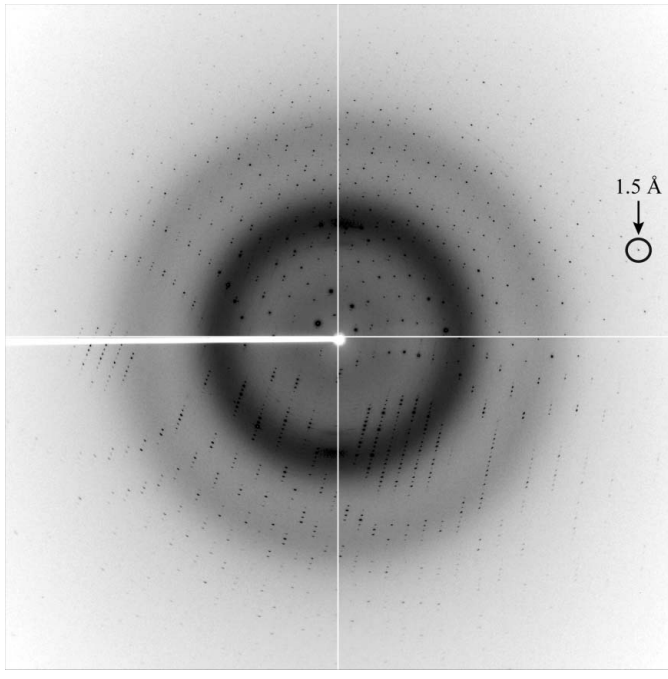

Figure 2
An X-ray diffraction image of the CALP–iCAL36 crystal. The black circle indicates a reflection at 1.5 Å resolution.

iCAL36 domain promises insights into the stereochemistry of a PDZ-selective peptide inhibitor.

We thank Abigail Fellows for technical assistance, Dr James Féthière (University of Montreal) for advice and Drs Vivian Stojanoff and Jean Jakoncic (NSLS) for assistance with data collection and analysis. Funding support was provided by the NIH (grants R01-DK075309 and P20-RR018787 and predoctoral fellowships to JFA and PRC from T32-GM008704) and the Cystic Fibrosis Foundation Research Development Program (STANTO97R0).

References

Adams, P. D. *et al.* (2010). *Acta Cryst.* D**66**, 213–221.
Cheng, J., Moyer, B. D., Milewski, M., Loffing, J., Ikeda, M., Mickle, J. E., Cutting, G. R., Li, M., Stanton, B. A. & Guggino, W. B. (2002). *J. Biol. Chem.* **277**, 3520–3529.
Cushing, P. R., Fellows, A., Villone, D., Boisguérin, P. & Madden, D. R. (2008). *Biochemistry*, **47**, 10084–10098.
Cushing, P. R., Vouilleme, L., Pellegrini, M., Boisguérin, P. & Madden, D. R. (2010). *Angew. Chem. Int. Ed. Engl.* **49**, 9907–9911.
Daniels, D. L., Cohen, A. R., Anderson, J. M. & Brünger, A. T. (1998). *Nature Struct. Biol.* **5**, 317–325.
Guggino, W. B. & Stanton, B. A. (2006). *Nature Rev. Mol. Cell Biol.* **7**, 426–436.
Harris, B. Z. & Lim, W. A. (2001). *J. Cell Sci.* **114**, 3219–3231.
Hillier, B. J., Christopherson, K. S., Prehoda, K. E., Bredt, D. S. & Lim, W. A. (1999). *Science*, **284**, 812–815.
Im, Y. J., Lee, J. H., Park, S. H., Park, S. J., Rho, S.-H., Kang, G. B., Kim, E. & Eom, S. H. (2003). *J. Biol. Chem.* **278**, 48099–48104.
Kabsch, W. (2010). *Acta Cryst.* D**66**, 125–132.
Kantardjieff, K. A. & Rupp, B. (2003). *Protein Sci.* **12**, 1865–1871.
Li, X., Zhang, J., Cao, Z., Wu, J. & Shi, Y. (2006). *Protein Sci.* **15**, 2149–2158.
Long, F., Vagin, A. A., Young, P. & Murshudov, G. N. (2008). *Acta Cryst.* D**64**, 125–132.
Luft, J. R., Collins, R. J., Fehrman, N. A., Lauricella, A. M., Veatch, C. K. & DeTitta, G. T. (2003). *J. Struct. Biol.* **142**, 170–179.
McCoy, A. J. (2007). *Acta Cryst.* D**63**, 32–41.
Nourry, C., Grant, S. G. & Borg, J. P. (2003). *Sci. STKE*, **2003**, re7.
Piserchio, A., Fellows, A., Madden, D. R. & Mierke, D. F. (2005). *Biochemistry*, **44**, 16158–16166.
Sugi, T., Oyama, T., Muto, T., Nakanishi, S., Morikawa, K. & Jingami, H. (2007). *EMBO J.* **26**, 2192–2205.
Vouilleme, L., Cushing, P. R., Volkmer, R., Madden, D. R. & Boisguerin, P. (2010). *Angew. Chem. Int. Ed. Engl.* **49**, 9912–9916.
Wolde, M., Fellows, A., Cheng, J., Kivenson, A., Coutermarsh, B., Talebian, L., Karlson, K., Piserchio, A., Mierke, D. F., Stanton, B. A., Guggino, W. B. & Madden, D. R. (2007). *J. Biol. Chem.* **282**, 8099–8109.
Zhang, Y., Appleton, B. A., Wiesmann, C., Lau, T., Costa, M., Hannoush, R. N. & Sidhu, S. S. (2009). *Nature Chem. Biol.* **5**, 217–219.